as a measure of soiling potential (*9*), implies over 50 percent greater soiling by the aerosol of the unleaded fleet, apparently because of the presence of carbonaceous particles.

These field tests, conducted under the maximum practicable degree of realism with respect to car operation and fuel choices, confirm the inference from the laboratory tests of Habibi *et al.* (*3*) that the use of current commercial unleaded fuels in present-day cars would lead to an increased output of carbonaceous particles, resulting in greater soiling and reduced atmospheric clarity. The observed near-doubling of the extinction coefficient under what is equivalent to heavy traffic conditions (calculated average CO concentration, ~ 15 parts per million) corresponds to reducing by half the visual range of lights or of prominent dark objects commonly used as daytime visibility markers. These results point up the complexity of the issue of the removal of lead from gasolines and the need for careful consideration of the consequences of such action.

JOHN M. PIERRARD
Petroleum Laboratory, E. I. du Pont de Nemours & Company, Wilmington, Delaware 19898

References and Notes

1. A measure of atmospheric clarity is the meteorological range, L_V, computed from the extinction coefficient, b_{ext}, by means of the formula $L_V = 3.9/b_{ext}$ for an assumed 2 percent contrast threshold [W. E. K. Middleton, *Vision through the Atmosphere* (Univ. of Toronto Press, Toronto, 1952), pp. 103–105]. In urban atmospheres, the contributions of molecular scattering and absorption to extinction can, in general, be ignored [R. J. Charlson, *Environ. Sci. Technol.* **3**, 913 (1969)]. It is also customarily assumed, in lieu of adequate measurements, that the extinction component due to absorption by aerosol particles is negligible, whence the expression for meteorological range depends only on the scattering coefficient of the aerosol particles, b_{scat}, namely, $L_V = 3.9/b_{scat}$. There is indirect experimental justification for this assumption [H. Horvath and K. Noll, *Atmos. Environ.* **3**, 543 (1969)].
2. R. J. Charlson and J. M. Pierrard, *Atmos. Environ.* **3**, 479 (1969).
3. K. Habibi, E. S. Jacobs, W. G. Kunz, Jr., D. L. Pastell, paper presented at the fifth technical meeting, West Coast section, Air Pollution Control Association, San Francisco, 1970.
4. J. M. Pierrard and R. A. Crane, *Hydrocarbon Process.* **50**, 142 (1971).
5. "An Economic Analysis of Proposed Schedules for Removal of Lead Additives from Gasoline," (Bonner and Moore Associates, Houston, 1971); S. Field, *Hydrocarbon Process.* **50**, 147 (1971).
6. U.S. Department of Health, Education, and Welfare, *Fed. Regist.* **33**, part 2 (No. 2), 116 (1968).
7. N. C. Ahlquist and R. J. Charlson, *J. Air Pollut. Contr. Ass.* **17**, 467 (1967); ———, H. Selvidge, P. B. MacCready, Jr., *ibid.* **19**, 937 (1969).
8. J. R. Sabina, J. J. Mikita, M. H. Campbell, *Proc. Amer. Pet. Inst.* **33**, 137 (1953); A. O. Melby, D. R. Diggs, B. M. Sturgis, *Soc. Automot. Eng. Trans.* **62**, 32 (1954).
9. Report No. 17913 of the Working Party, "Methods of Measuring Air Pollution" (Organisation for Economic Co-operation and Development, Paris, 1965).
10. It is assumed that molecular scattering and absorption are negligible, so that the extinction coefficient is the sum of the aerosol scattering and absorption coefficients. The increase in the extinction coefficient is the difference between the final extinction coefficient, computed by Beer's law from the transmittance measured after 24 cycles of driving, and the initial extinction coefficient, assumed to be equal to the initial scattering coefficient; the increase in the scattering coefficient is the difference between the final average scattering coefficient (over the same path viewed by the transmissometer) computed from the nephelometer traverse record and the initial scattering coefficient; the increase in the absorption coefficient is the difference between the increases in the extinction and scattering coefficients. Only the lower limit of the increase in the scattering coefficient was determinable from one of the four tests with each fleet. But, since the increase in the scattering coefficient can be no greater than the increase in the extinction coefficient, the ranges of mean increase of scattering and absorption coefficient were calculable.
11. I thank the Pennsylvania Turnpike Commission for the use of the Sideling Hill tunnel, and my colleagues at Du Pont for their assistance in this work.

20 September 1971; revised 11 November 1971 ■

Population Modeling: A Systems Approach

Abstract. *A single species population dynamics model based on the functional representations of birth, growth, and death has been constructed. Laboratory parameter estimates were used in a computer implementation of the model to simulate field populations. Preliminary results of replicate runs with parametric sampling indicated reasonable statistical agreement. Further development with the systems analysis technique is planned.*

Mathematical modeling has brought about revolutionary advances in the physical sciences. One aspect of modeling is the elucidation of the essence of a system, to provide better understanding of the complexities of its natural behavior. Faced with the vast variability present in ecosystems, engineers, biologists, and other scientists can benefit from application of mathematical modeling techniques. Several guidelines for modeling systems should be considered.

1) Initially, the scientist must define the problem, distinguishing it from the rest of the surrounding universe. We choose the problem as the study of the population dynamics of a single species and the universe as everything else. The level of organization selected reflects the degree of resolution desired.

2) The next step is the selection of system components. The component must be a coherent entity at a lesser level of organization than the problem at large. For convenience a good first guess is that the components should be the largest coherent subsets which, when combined, capture the essence of the problem.

The best set of components, although not unique, will be that set which reflects the primary functional characteristics of the modeling problem. A production-ecologist might lump species populations into functional arrays (producers, consumers, and the like) as his components. The functions to be modeled dictate the selection of components.

In this single species model of population dynamics the primary functional considerations are birth, growth, death, and temperature effects. While individual instars (life stages) readily suggested themselves as system components, functional considerations challenged this approach. The homogeneity of rate functions of the first six instars of the freshwater shrimp *Hyalella azteca* led to the grouping of these six into one component. Each of the remaining six instars were sufficiently variable to consider each of them as a separate component. These breakdowns were strictly on the basis of functional discreteness.

3) Each individual component must be given a free body characterization. The component is given a mathematical description which interrelates the inputs, outputs, and states of the system. The component is considered as a discrete package in its entirety. It is in this procedure that the biological intuition and understanding is incorporated into strict mathematical formalisms. Any gross assumptions or simplifications concerning either the biology or the mathematics must be made explicit.

The state variables must be chosen so that they encapsulate the functions of the component. In a population dynamics model, in which grouped instar components are used to generate numerical changes in population size, the state variable can be population size. There must be a relation between the terminal (input-output) variables and the state variables. These relations must be the essence of the component in isolation.

4) The linkage of components is essentially simple. The outputs of one become the inputs to other components. This does not necessarily infer a tem-

poral ordering—that is, births from adult classes provide the input to the young stage.

5) Once the components are coupled to each other, they still must be linked to the universe (their environment). This new linkage constrains the behavior of the isolated system, much as the connections within the system constrain the individual components. These handles to the universe are routes by which the system under study influences and is influenced by events external to it.

Experimentation is necessary to furnish the parameters of the model. Real world values are then assigned to the system variables. The model is then carefully tuned and experimentally validated.

Our model is essentially a single species population dynamics model. It is based on a life table approach (*1*) and contains all the parameters of natural population growth: birth, growth, and death. Most previous models are based purely on mathematical techniques. Our model, in contrast, is based on the mathematical representation of biological functions. The model has several important features as follows.

1) It chronicles class specific rate functions. These classes may be according to age, size, or instar. This allows for class differences. It can be shown to be similar in structure to the models of Sinko and Streifer (*2*).

2) Instead of single estimates of given parameters, a range of naturally occurring values are used. Thus, the genetic variability of natural populations is reflected in the structure of the model. This captures the variability between populations, rather than that between individuals.

3) It is a predictive model that generates a mean predictor with an estimate of variance. This is based on the above-mentioned variability in the parameters. One prediction is generated (that is, the size distribution of the population after t days). Next, the random selection of parameter occurs again, and a new prediction is generated. The results are averaged, and a variance is computed. This generates a mean predictor with a specified range of reliability.

4) Having a mean and variance of the prediction creates the fourth property of the model. Its predictions can be tested by many statistical techniques.

5) The structure of the model is generally applicable to many animal and plant species.

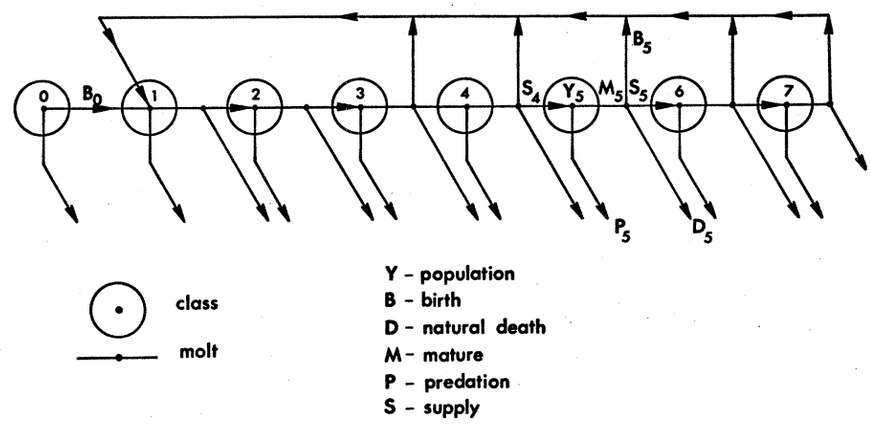

Fig. 1. The complete model structure for the amphipod *Hylella azteca*.

The fundamental component is defined on a functional basis, perhaps by size, age, or instar, depending on the emphasis of the model. The guideline here is homogeneity of the relevant functions. The structure of this building block is illustrated for Y_5 in Fig. 1. It reflects the coupling structure, the class population, and the molt functions of natural death, birth, and class transition. These functions, as well as predation, are class specific, as is the duration of the class. Important, but not explicitly seen, is the age distribution of the intraclass population.

With these comments as background we can formally state the model structure mathematically (Eqs. 1 to 6). We have chosen a discrete time form. This concept is usually the most lucid to nonspecialists in analysis. We are not including diurnal rhythms, and the unit of 1 day appears most useful for census and function rates. A simple daily census balance may be written. The basic functional representations are proposed for the ith class. The symbols are as follows: Y, population; B, birth; D, natural death; M, maturation; P, predations; S, supply; n, day; p_i, fraction lost to predation; d_i, fraction lost to natural death; b_1, brood size ratio of the number of young to the number of adults. The unit for all capital letter symbols is number of individuals.

$$Y_i(n+1) = Y_i(n) + S_{i-1}(n) - P_i(n) - M_i(n) \quad (1)$$

$$P_i(n) = p_i(n)\, Y_i(n) \quad (2)$$

$$M_i(n) = \sum_{j=0}^{\eta(T)-1} [1 - p_i(n-j)]S_{i-1}[n - \eta(T)] \quad (3)$$

$$D_i(n) = d_i(n)\, M_i(n) \quad (4)$$

$$S_i(n) = M_i(n) - D_i(n) \quad (5)$$

$$B_i(n) = b_i(n)\, S_i(n) \quad (6)$$

The implication of maturation M_i and class life period $\eta(t)$ deserves special attention. The value of $\eta(T)$ is the duration in days of the ith class. It is explicitly a function of environmental temperature (T). The number that enter a class i at time $n - \eta(T)$ is S_{i-1} $[n - \eta(T)]$. The number maturing at time n, namely $M_i(n)$, are those individuals from this group which remain, having survived the effects of predation over the past $\eta(T)$ days. This implies that several days recruits could mature on the same day. Since the duration of the class is dependent on temperature, variation in growth rate can result. In view of the lack of data, p_i, b_i, and d_i were taken as constants. Two environmental couplings (p_i, T) are now explicit in the model.

One special component is needed for the seasonal animal, namely an initial source. Overwintering adults provide this (Eqs. 2, 7, and 8) in our work. A population birth rate is used here as a result of available data and population homogeneity.

$$Y_0(n+1) = Y_0(n) - P_0(n) \quad (7)$$

$$B_0(n) - b_0\, Y_0(n) \quad (8)$$

The coupling equations are implied in the class index except for recruitment into class two, the newborn. This is given in Eq. 9.

$$S_0(n) = \sum_{i=0}^{k} B_i(n) \quad (9)$$

where k is the number of classes. Such simple couplings may not always be the case, and the nomenclature may need slight adjustment. Several computational manipulations are required to generate the solution to the model.

Parameters were chosen for the model and validated using the freshwater amphipod *Hyalella azteca* Saus-

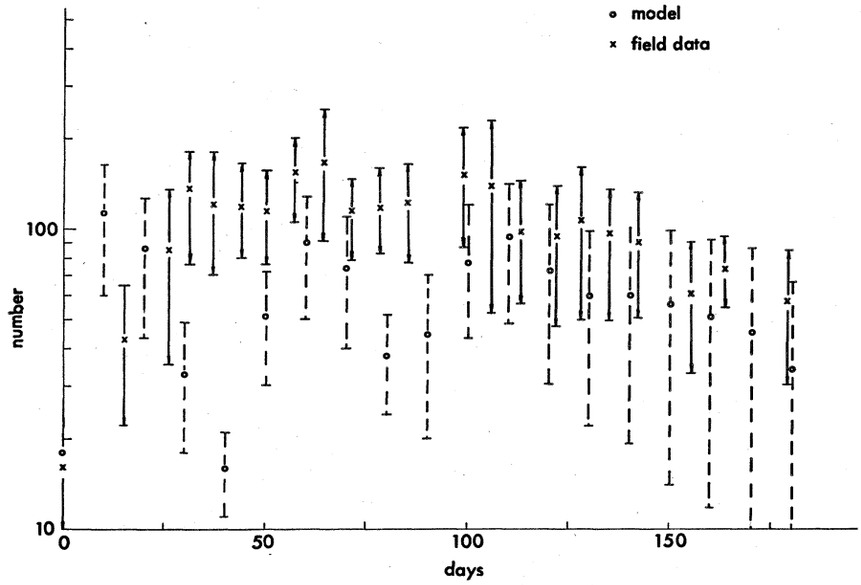

Fig. 2. Results for the 1- to 6-instar class.

sare (*4*). W. E. Cooper has written the definitive monograph on *H. azteca* (1965) and provided unpublished data and suggestions. Reice had extensive field and laboratory experience with the amphipod. However, the overriding considerations in the choice were ecological; *H. azteca* is a crustacean, a free-swimming benthic scavenger. A major part of its feeding consists in bacterial and fungal grazing (*5*). It progresses through a series of discrete instars with the main mortality (excluding predation) occurring at the moults (*6*). For the model, the 12 instars have been grouped by homogeneity of parameters. The large body of information on *H. azteca* includes population parameter estimates in the laboratory and in the field. Much is known about predation patterns, feeding, and temperature responses. The young are born live, and the brood size of the adult instars is a function of body size. In addition, the growth rate is a function of temperature.

The model, at this stage, assumes that there is a superabundance of food —hence no food limitation or competition qualities are included. Predation by fish is size specific (*7*). This holds true for *H. azteca*. Therefore, predation has been weighted toward larger individuals

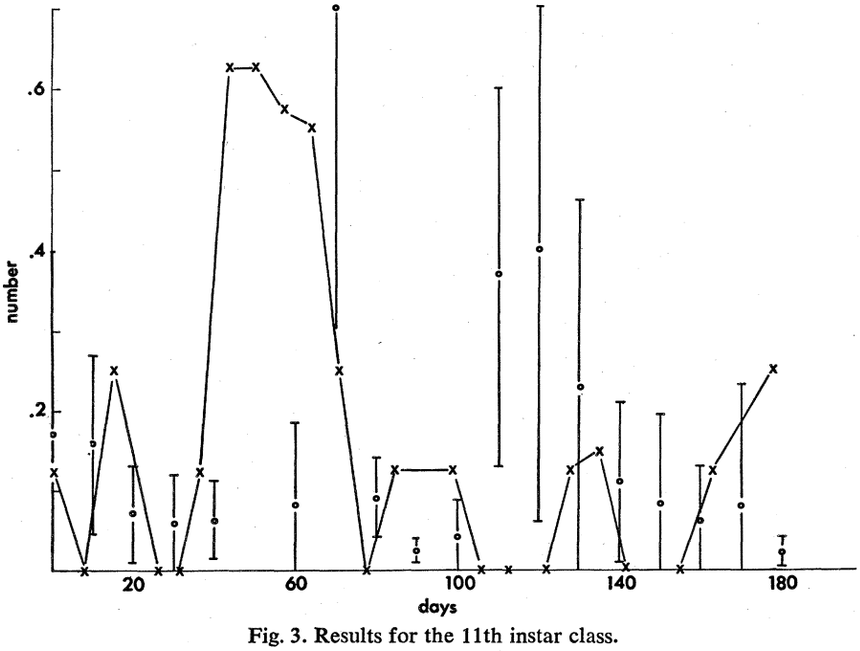

Fig. 3. Results for the 11th instar class.

In all, *H. azteca* is an ideal animal for the study of population dynamics. It lends itself to clear interpretation of life history phenomena and parameter estimation.

The parameters of the model were drawn from the laboratory data of Cooper (*6*). All parameter values were assumed to be normally distributed with the standard deviation set at 25 percent of the mean. The 20°C life table values were taken as the mean for each of the parameters. The predation parameters (p_0 to p_7) were derived from Cooper's analyses of fish gut.

The predictions of the model were tested against Cooper's field data. The model was tested in replicate with the laboratory-based parameters. Values for parameters were chosen at random from the appropriate probability density functions. Thus each test had a different set of parameter values. The same temperature data as that in Cooper's field work was used. Mean predictors and variances for each size class on each day were obtained. The results, comparing the predictions of the model ($\bar{x} \pm$ S.D.) and the field measures ($\bar{x} \pm$ S.D.) are below (Figs. 2 and 3). Owing to the vast amount of data, only two representative classes are shown, the 1- to 6-instar class and the 11th class. Cooper's data is presented as is. The model's predictions are given for every tenth day, for clarity of visual presentation. The predictions of the model form an envelope of possible conditions (within 1 S.D. to either side of the mean). The relative success of the model may be assessed by the degree of overlap of the variances of the data and the predictions. The model is too rough to justify a detailed statistical analysis of the results. At this stage of development the predictability appears to be reasonable. Future refinements are necessary to generate more precise results.

The basic value of the single species population dynamics model itself is that it is predictive. The model is based on many of the biological realities of a species. It uses independent laboratory estimates of parameters to generate predictions in the field. The most important shortcoming is that it cannot handle feeding behavior, concomitant competition, and its influence on popuplation dynamics. Building this in is the obvious next step. Several interesting paths of analytical development are suggested by the mathematical structure of the model. These principally concern stochastic processes and stability analysis. In sum,

the single species model has opened one avenue for delving into community and ecosystem problems through the modeling approach of systems analysis.

G. A. COULMAN
Department of Chemical Engineering, Michigan State University, East Lansing 48823

S. R. REICE
Department of Zoology, Michigan State University

R. L. TUMMALA
Division of Engineering Research, Michigan State University

References and Notes

1. A. J. Lotka, *Elements of Mathematical Biology* (Dover, New York, 1956); G. F. Gause, *The Struggle for Existence* (Hafner, New York, 1939); L. C. Birch, *J. Anim. Ecol.* **17**, 15 (1948); F. C. Evans and F. E. Smith, *Amer. Nat.* **86**, 299 (1952).
2. J. W. Sinko and W. Streifer, *Ecology* **48**, 910 (1967); *ibid.* **50**, 608 (1969).
3. Details of the computation may be obtained from G. A. Coulman.
4. R. W. Pennak, *Fresh Water Invertebrates of the United States* (Ronald, New York, 1953).
5. B. T. Hargrave, *J. Anim. Ecol.* **39**, 427 (1970).
6. W. E. Cooper, *Ecol. Monogr.* **35**, 377 (1965).
7. J. L. Brooks and S. I. Dodson, *Science* **150**, 28 (196 → M. C. Galbraith, Jr., *Trans. Amer. Fish. Soc.* **96**, 1 (1967); J. L. Brooks, *Syst. Zool.* **17**, 273 (1968).
8. Supported by NSF grant GI-20.

1 June 1971; revised 27 September 1971 ■

Crystallization Studies of Lunar Igneous Rocks: Crystal Structure of Synthetic Armalcolite

Abstract. *Crystals of armalcolite, $Mg_{0.5}Fe_{0.5}Ti_2O_5$, up to several millimeters in length have been grown from a glass initially having the composition of lunar rock 10017. A single-crystal x-ray study has confirmed that the crystals are isomorphous with pseudobrookite and has shown that the cations are strongly ordered, with the Ti^{4+} ions occupying the 8f sites and the Fe^{2+} and Mg^{2+} ions randomly distributed over the 4c sites. An examination of karrooite, $MgTi_2O_5$, has revealed a similar distribution of Mg^{2+} and Ti^{4+} ions. A reexamination of earlier x-ray and Mössbauer data for pseudobrookite, Fe_2TiO_5, has shown that it is more consistent with this type of ordering than with the inverse structure that has been generally assumed.*

During an investigation of the feasibility of studying the crystallization of lunar igneous rocks by high-temperature x-ray diffractometer techniques, we have obtained black needle-like crystals that have proved to be the mineral armalcolite, $Mg_{0.5}Fe_{0.5}Ti_2O_5$, recently discovered in the Apollo 11 lunar samples (*1*). Many of these crystals are several millimeters long and several tenths of a millimeter in cross section and lie in the surface of the solidified melt; thus, sections can be removed that are ideal for investigation of the structure by single-crystal x-ray techniques. We have also grown and studied crystals of the isomorphous mineral karrooite, $MgTi_2O_5$. We have found that the distribution of cations in these crystals is the inverse of that proposed for the isomorphous mineral pseudobrookite, Fe_2TiO_5 (*2, 3*). A reconsideration of x-ray (*2, 3*) and Mössbauer (*4*) data on pseudobrookite has led us to conclude that the previously proposed cation arrangement is probably incorrect.

The starting material for our crystallization studies, a glass corresponding closely in composition to lunar rock 10017 (*5*), was prepared from pure oxides, Fe metal, and synthetic anorthite ground together and pressed into pellets. The mixture was melted with an induction furnace in a closed Fe crucible in an Ar atmosphere, and after several hours above the liquidus temperature was "quenched" by turning off the power. Microscopic examination showed occasional small octahedrons of metallic Fe to be the only crystalline phase present.

Four experiments at high temperature were made in a Materials Research model X-86-G2 furnace; the powder x-ray diffractometer was General Electric model XRD-5. In each experiment a few milligrams of powdered glass (particle size less than 44 μm) in an acetone slurry was put on the heater strip of the furnace. In one experiment a heater made of Pt with 40 percent Rh was used and the sample volume was continuously pumped to maintain a total pressure of about 10^{-5} mm of Hg. In the other experiments Mo strips were used, in one case pumped as above, then with flowing He at 10^{-4} mm of Hg, and finally with flowing H_2 at 10^{-3} mm of Hg. In each case the temperature of the heater was raised until the sample spread over the strip as a smooth film and then lowered in steps of about 25°C. At each temperature the x-ray powder pattern was recorded with MoKα radiation. In all cases armalcolite was the first phase to crystallize, and it remained stable as the temperature was gradually lowered to about 1000°C, at which point the sample was fairly rapidly cooled to room temperature. No ilmenite formed during these experiments.

In lunar rock 10017 ilmenite is abundant while no armalcolite is found. The same is true of the synthetic 10017 melt when it is cooled in an Fe crucible in an inert atmosphere. In the case of the experiment on Pt–(40 percent)-Rh, loss of Fe from the melt was evidenced by bubbling and the formation of a clear glass layer next to the strip. Although it was expected that loss of Fe would be less severe on the Mo strips (*6*), and such obvious evidence of loss was not seen there, the

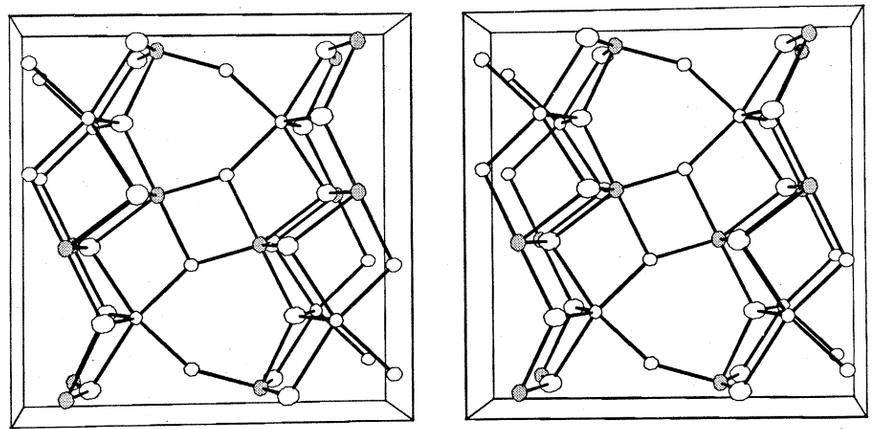

Fig. 1. Stereoscopic view of the contents of one unit cell of armalcolite. The viewing direction is along the *c* axis. The cations in 8*f* sites are shaded. The ellipsoids indicating the thermal motion probability are scaled to include 75 percent probability.